PROCEEDINGS OF THE ROYAL SOCIETY A

Proc. R. Soc. A (2008) **464**, 3021–3038
doi:10.1098/rspa.2008.0136
Published online 10 July 2008

Double cavity flow past a wedge

By Y. A. Antipov[1,*] and V. V. Silvestrov[2]

[1]*Department of Mathematics, Louisiana State University, Baton Rouge, LA 70803, USA*
[2]*Department of Mathematics, Gubkin Russian State University of Oil and Gas, Moscow 119991, Russia*

A mathematical model of supercavitating flow past a wedge with sides of arbitrary length is proposed. The flow branches at a point on the lower side of the wedge. At the vertex of the wedge and at the ends of the wedge, the flow breaks away forming a nose bubble and a trailing cavity. The closure mechanism is described by the Tulin single-spiral-vortex model. The flow domain is mapped into a parametric plane cut along a unit segment. The conformal mapping function is reconstructed through the exact solution of two Riemann–Hilbert problems on a genus-zero Riemann surface. To complete the solution, one needs to determine five real parameters from a certain system of transcendental equations. Numerical results are presented for the case when a wedge can rotate about the vertex in the flow domain. In this case, the flow branches at the vertex and the number of the parameters to be determined is 3.

Keywords: Riemann–Hilbert problem; conformal map; cavitation

1. Introduction

One of the central problems in hydrodynamic cavitation modelling is the study of supercavitating flow (the cavity closes away from a hydrofoil). The modelling of supercavitation is based on the results by Brillouin (Birkhoff & Zarantello 1957), who proved that the maximum speed must be attained on the free surface and also that the boundary of a cavity is convex. For an inviscid fluid in irrotational flow, all known steady models first assume that the speed is prescribed and constant on the boundary of a cavity that is a streamline of the flow and, second, that the cavity is not closed. The assumption that the free streamlines close in a bounded domain results in a stagnation point within a cavity. This is inconsistent with the condition of constant pressure within the cavity. The impossibility of the cavity modelling by a closed domain is known as the Brillouin paradox. This paradox follows from the assumption that the flow is steady. However, the flow is transient mostly in the rear part of the cavity. To describe the mechanism of the cavity closure, several supercavitating flow models were proposed in the past (Birkhoff & Zarantello 1957; Eisenberg & Tulin 1961; Wu 1972; Gurevich 1979; Brennen 1995; Frank & Michel 2004).

A single-spiral-vortex model was proposed by Tulin (1964), and it was further developed by Terent'ev (1976). The flow in the rear part of the cavity can be considered as the flow on a half of an infinitely sheeted Riemann surface of the

* Author for correspondence (antipov@math.lsu.edu).

Received 2 April 2008
Accepted 17 June 2008

logarithmic function with two branch points, say, C^+ and C^-. The streamline that branches at the surface of the body branches again at a point C at the rear part of the cavity. The streamlines that are close to the boundary of the cavity traverse first around the cavity and then pass to the Riemann surface. After they have traversed a finite number (unknown *a priori*) of the sheets of the Riemann surface, the streamlines return to the points $C^{\pm}$ on the first sheet where the body is placed. Mathematically, this model of the cavitating flow admits the presence of a singularity of the solution at the point C, where the two branches of the streamline attempt to close the cavity,

$$\log(\mathrm{d}w/\mathrm{d}z) \sim K(w-w_0)^{-1/2}, \quad z \to \mathrm{C}, \quad K = \text{const}. \tag{1.1}$$

Here, $w_0 = w(\mathrm{C})$ and $w = w(z)$ is the complex potential of the flow. This condition extends the class of solutions to the governing boundary-value problem that makes it possible to reconstruct a flow that meets the necessary condition $\oint_L \mathrm{d}z = 0$ (L is the boundary of the cavity combined with the boundary of the hydrofoil).

In the case of simply and doubly connected domains, the nonlinear steady model problems of the cavitating flow can be solved analytically by mapping a hodograph plane into the flow domain (Birkhoff & Zarantenello 1957; Gurevich 1979). A free boundary problem for a triply connected domain can be reduced (Cherepanov 1964) to a Riemann–Hilbert problem with a piece-wise constant coefficient along the real axis. Recently, a closed-form solution technique was proposed (Antipov & Silvestrov 2007) for a nonlinear supercavitating flow around two plates in a channel with a free boundary. The method maps a parametric plane with three cuts on the real axis into the flow domain and requires the solution of a Riemann–Hilbert problem on a Riemann surface of genus 2. The method developed is applicable for either $(n+1)$-connected domains, when $0 \leq n \leq 2$, or the linearized models for any finite n, when all the foils are placed in a plane on the same axis. The main difficulty in the implementation of the method is to evaluate singular integrals on the Riemann surface and find the parameters of the conformal mapping from a system of transcendental equations.

In this paper, we analyse a supercavitating potential flow past a wedge. The flow branches at some point on the lower side of the wedge. Owing to the inability of the real fluid to go around sharp corners without breaking away from the corner, we assume the existence of a partial cavity or a nose bubble. The model also assumes that the branched streamline breaks away from the wedge at the ending points. At some point behind the wedge, the branches of the streamline attempt to merge, forming thus a trailing cavity. Note that Cox & Clayden (1958) also considered a double cavity model for a wedge. In their case, the wedge was assumed to be symmetric, the partial cavity was described by the re-entrant-jet Kreisel–Efros model, while for the trailing cavity, they used the Kirchhoff model.

2. Formulation

Consider a model problem of a steady flow past a wedge DAB (figure 1). The velocity of the stream at infinity is $\boldsymbol{v} = (V_\infty, 0)$, the angles that the segments AB and AD make with the horizontal axis are α and β ($\alpha \leq \beta$), respectively, and $|\mathrm{AB}| = \lambda_1$ and $|\mathrm{AD}| = \lambda_2$. The flow is assumed to be potential and the viscosity and the gravity are neglected. Let the stagnation point, A_0, be located somewhere

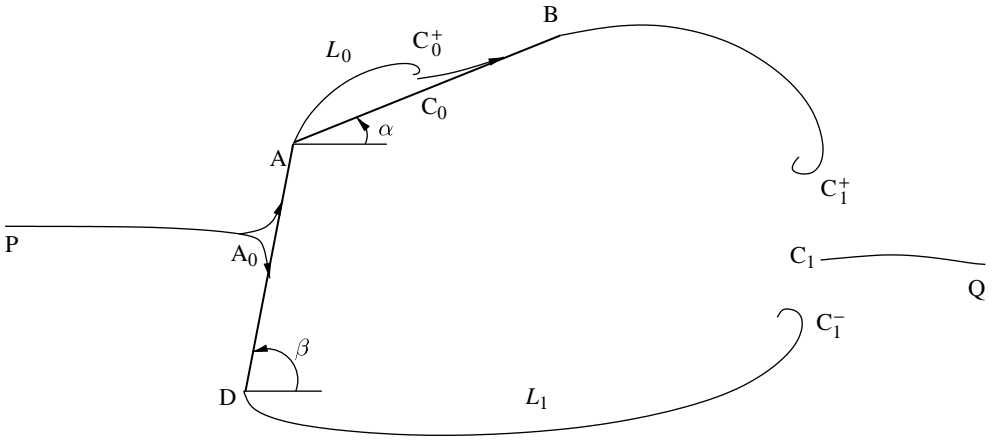

Figure 1. Double cavity flow past a wedge.

on the lower face AD of the wedge. Then, the flow branches at the point A_0, and the upper streamline traverses the upper part A_0A of the face AD. Owing to the inability of the real fluid to go around sharp corners without breaking away from the corner (it requires an infinite flow velocity otherwise), we assume the existence of a partial cavity or a nose bubble AC_0^+. The lower branch $A_0DC_1^-$ of the streamline PA_0 traverses the segment A_0D, breaks away from the wedge and attempts to join the upper branch $C_0^+BC_1^+$ of the same streamline at a point C_1 behind the wedge forming a trailing cavity. Both the cavities are bounded but not closed and a smooth detachment of the cavities at the points A, B and D is assumed. To describe the cavity closure mechanism, the Tulin single-vortex model is used. Apart from small neighbourhoods of the points C_0^+, C_1^+ and C_1^-, the cavities are convex. On account of the Bernoulli equation, the speeds, V_0 and V_1, of the flow on the cavity boundaries $L_0 = AC_0^+$ and $L_1 = BC_1^+C_1^-D$ are constant: $V_j = \sqrt{\kappa_j + 1}\, V_\infty$, $j{=}0, 1$, where κ_0 and κ_1 are the prescribed cavitation numbers of the nose bubble L_0 and the trailing cavity L_1, respectively.

To write down the mathematical formulation, we use the complex velocity potential $w(z) = \phi(z) + \mathrm{i}\psi(z)$, where $z = x + \mathrm{i}y \in \mathcal{D}$; $\mathcal{D}$ is the flow domain; ϕ is the velocity potential; and ψ is the stream function. The velocity vector $\boldsymbol{v} = (u_x, u_y)$ is given by $(\mathrm{d}w/\mathrm{d}z) = u_x - \mathrm{i}u_y = V\,\mathrm{e}^{-\mathrm{i}\theta}$, where $V = |\mathrm{d}w/\mathrm{d}z|$ is the flow speed and $\theta = -\arg(\mathrm{d}w/\mathrm{d}z)$ is the angle that the velocity vector makes with the x-axis. The function $w(z)$ is analytic in the flow domain $\mathcal{D}$ and it satisfies the following boundary conditions:

$$\operatorname{Im} w(z) = K, \quad z \in L_0 \cup C_0B \cup L_1 \cup DA, \quad K = \text{const.}$$

and

$$\left|\frac{\mathrm{d}w}{\mathrm{d}z}\right| = V_j, \quad z \in L_j, \quad j = 0, 1, \quad \arg\frac{\mathrm{d}w}{\mathrm{d}z} = \begin{cases} -\alpha, & z \in C_0B, \\ -\beta, & z \in A_0A, \\ \pi - \beta, & z \in A_0D. \end{cases} \tag{2.1}$$

The flow domain $\mathcal{D}$ is simply connected, and the solution to the nonlinear problem (2.1) is very much aided by mapping the entire boundary, $\partial\mathcal{D}$, of the flow into the exterior of the unit segment in a parametric plane. Let $z{=}f(\zeta)$ be

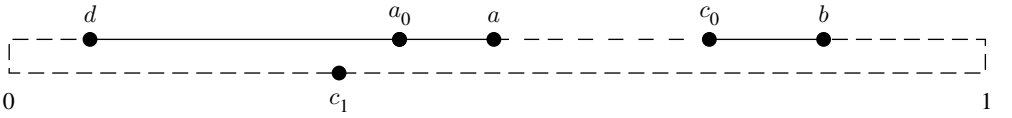

Figure 2. Parametric ζ-plane cut along the segment l.

a conformal map of a parametric ζ-plane cut along the unit segment, $l=[0,1]$, of the real axis onto the flow domain $\mathcal{D}$. Such a map is defined up to three real parameters. By assuming that the infinite point of the physical domain maps into the infinite point of the parametric plane, we fix the first two parameters. By letting the vertex A fall into the point $a=(1/2)+\mathrm{i}0$, we fix the third parameter and thus define the map uniquely. The boundary points C_0, B, C_1, D and A_0 are mapped into the points c_0, b, c_1, d and a_0 of the cut l, respectively.[1] The two distinct points C_0^+ and C_0 and the three points C_1^+, C_1 and C_1^- of the flow domain are mapped into the two single points c_0 and c_1 of the cut l. The points a, c_0, b, c_1, d and a_0 follow each other in the clockwise direction. All these points, apart from the point $a=(1/2)+\mathrm{i}0$, are to be determined. The image pattern of the flow domain by the inverse transform $\zeta=f^{-1}(z)$ is shown in figure 2. The solid line corresponds to the solid boundary of the flow and the dashed line is the image of the unknown curves.

In order to obtain the requisite conformal mapping function $z=f(\zeta)$ and to solve the problem, it is sufficient to find the derivatives $\mathrm{d}w/\mathrm{d}\zeta$ and $\mathrm{d}w/\mathrm{d}z$ and integrate the relation

$$\frac{\mathrm{d}f}{\mathrm{d}\zeta}=\frac{\mathrm{d}w/\mathrm{d}\zeta}{\mathrm{d}w/\mathrm{d}z}. \tag{2.2}$$

In the following, we write down two Riemann–Hilbert problems for the definition of the functions $\mathrm{d}w/\mathrm{d}\zeta$ and $\mathrm{d}w/\mathrm{d}z$. Instead of the derivative $\mathrm{d}w/\mathrm{d}z$, it will be more convenient to deal with the following function:

$$\omega(\zeta)=\log\frac{\mathrm{d}w(z)}{V_\infty\,\mathrm{d}z}=\log\frac{V}{V_\infty}-\mathrm{i}\theta,\quad z=f(\zeta). \tag{2.3}$$

The function $\omega(f^{-1}(z))$ is defined in the flow domain $\mathcal{D}$ cut along the streamline joining the infinite point with the stagnation point A_0.

The boundary conditions (2.1) imply that, on the cavity boundary, the real part of the function $\omega(\zeta)$ is prescribed as

$$\operatorname{Re}\omega(\zeta)=\begin{cases}\kappa_0', & \zeta\in ac_0,\\ \kappa_1', & \zeta\in bc_1d,\end{cases}\qquad \kappa_j'=\log\sqrt{\kappa_j+1},\quad j=0,1, \tag{2.4}$$

[1] Another possibility is to fix b and d by letting $b=1$ and $d=0$ and also to assume, for instance, that the point $z=\infty$ falls into a point, say, $\zeta_\infty\in(-\infty,0)\cup(1,\infty)$. Then, the point c_1 must be on the lower side l^- of the cut, and the other three points a_0, a and c_0 lie on the upper side of the cut. However, this leads to numerical difficulties due to a scaling problem: the numerical implementation of the method in the particular case $a_0=c_0=a$, for example, shows that the image ζ_∞ of the point $z=\infty$ is far away from the cut l, namely ζ_∞ is a real number of the order of 10^6–10^7.

while on the solid part of the boundary, the imaginary part is known as

$$\operatorname{Im}\omega(\zeta)=\begin{cases}-\alpha, & \zeta\in c_0b,\\ \pi-\beta, & \zeta\in da_0,\\ -\beta, & \zeta\in a_0a.\end{cases}\tag{2.5}$$

Since $\mathrm{d}w/\mathrm{d}z=0$ at $z=\mathrm{A}_0$, the function $\omega(\zeta)$ has a logarithmic singularity at the point $\zeta=a_0$. In a neighbourhood of the points c_0 and c_1, the function $\omega(\zeta)$ has the following singularity:

$$\omega(\zeta)\sim M_j'(w-w_j)^{-1/2},\quad z\to \mathrm{C}_j,\quad M_j'\neq 0,\tag{2.6}$$

where $w_j=w(\mathrm{C}_j)$, $j=0$, 1, and a single branch of the square root is considered in the w-plane cut along the axis $\arg(w-w_j)=\pi$. It can be shown (Antipov & Silvestrov 2007) that (2.6) implies $\omega(\zeta)\sim M_0''(\zeta-c_0)^{-1/2}$, $\zeta\to c_0$, and $\omega(\zeta)\sim M_1''(\zeta-c_1)^{-1}$, $\zeta\to c_1$, $M_j''\neq 0$, $j=0$, 1.

Next, define the boundary conditions for the function $\mathrm{d}w/\mathrm{d}\zeta$. It follows from (2.1) that

$$\operatorname{Im}\frac{\mathrm{d}w}{\mathrm{d}\zeta}=0,\quad \zeta\in l.\tag{2.7}$$

It is important to analyse the behaviour of the function $\mathrm{d}w/\mathrm{d}\zeta$ at the points a_0, c_0 and c_1. Let the points a_0, c_0 and c_1 not coincide with the ending points of the cut l. The main difference between the point C_0 from one side and the points A_0 and C_1 from the other side is that at the point C_0, two branches of the same streamline meet, and at the points A_0 and C_1, three branches meet. Therefore, the neighbourhoods of the points C_1 and A_0 that are locally semi-discs are mapped into discs with a cut in the w-plane (the hodograph plane), while a neighbourhood of the point C_0 (locally a quarter-disc) is mapped into a semi-disc in the w-plane. At the same time, the neighbourhoods of the three points A_0, C_0 and C_1 are mapped into semi-discs in the parametric ζ-plane. Thus,

$$w-w(\mathrm{C})\sim K(z-\mathrm{C})^2,\quad z\to\mathrm{C},\quad w\to w(\mathrm{C}),\quad K=\text{const},\tag{2.8}$$

where C is one of the points A_0, C_0 or C_1. On the other hand,

$$z-\mathrm{C}_0\sim K'(\zeta-c_0)^{1/2},\ \zeta\to c_0\ \text{ and }\ z-\mathrm{C}\sim K''(\zeta-c),\ \zeta\to c=a_0\text{ or }c_1.\tag{2.9}$$

It immediately follows from (2.8) and (2.9) that

$$\frac{\mathrm{d}w}{\mathrm{d}\zeta}\sim K_0,\quad \zeta\to c_0\quad\text{and}\quad \frac{\mathrm{d}w}{\mathrm{d}\zeta}\sim K_c(\zeta-c),\quad \zeta\to c=a_0\text{ or }c_1,\tag{2.10}$$

where K_0 and K_c are non-zero constants. Note that the function $\mathrm{d}w/\mathrm{d}\zeta$ is bounded and not equal to zero at any point of the set $\{a_0,c_1,c_0\}$ if that point coincides with one of the ending points. The point $\zeta=\infty$ corresponds to the point $z=\infty$ of the flow domain. Therefore, as $\zeta\to\infty$, $(\mathrm{d}w/\mathrm{d}\zeta)\sim\text{const.}\neq 0$. In a neighbourhood of the ending points $\zeta=0$ or 1 of the cut, if they do not coincide with the critical points a_0, c_0 or c_1, the function $\mathrm{d}w/\mathrm{d}\zeta$ admits the following representation: $(\mathrm{d}w/\mathrm{d}\zeta)\sim\hat{K}(\zeta-\hat{\zeta})^{-1/2}$; $\zeta\to\hat{\zeta}$; $\hat{\zeta}=0$; or 1; and $\hat{K}$ is a non-zero constant.

3. Riemann–Hilbert problems for the functions $\omega(\zeta)$ and $\mathrm{d}w/\mathrm{d}\zeta$

In this section, the two Riemann–Hilbert problems (2.4) and (2.5) for $\omega(\zeta)$ and (2.7) for $\mathrm{d}w/\mathrm{d}\zeta$ will be reduced to scalar Riemann–Hilbert problems on a Riemann surface.

(*a*) *Statement of the problem for the function* $\omega(\zeta)$

Let $\mathcal{R}$ be a genus-zero Riemann surface defined by the algebraic equation $u^2 = p(\zeta)$, $p(\zeta) = \zeta(1-\zeta)$. The surface is formed by gluing two copies C_1 and C_2 of the extended complex ζ-plane $\mathrm{C}\cup\{\infty\}$ cut along the segment l. The positive side l^+ of the cut $l\subset\mathrm{C}_1$ is glued to the negative side l^- of the cut $l\subset\mathrm{C}_2$, and the side $l^-\subset\mathrm{C}_1$ is glued to $l^+\subset\mathrm{C}_2$. The function $u(\zeta)$ is single valued on $\mathcal{R}$,

$$u = \begin{cases} p^{1/2}(\zeta), & \zeta\in\mathrm{C}_1,\\ -p^{1/2}(\zeta), & \zeta\in\mathrm{C}_2. \end{cases} \tag{3.1}$$

Here, $p^{1/2}(\zeta)$ is the branch fixed by the condition $p^{1/2}(\xi+\mathrm{i}0)>0$, $0<\xi<1$. The pair $(\zeta, p^{1/2}(\zeta))$ denotes a point on C_1 with affix ζ, while the notation $(\zeta,-p^{1/2}(\zeta))$ will be used for its counterpart on the second sheet. The sides of the cut l form the symmetry line for the surface $\mathcal{R}$ that splits the surface into two symmetric halves.

The Riemann–Hilbert problem (2.4) and (2.5) for the function $\omega(\zeta)$ may be formulated as a boundary-value problem on the Riemann surface $\mathcal{R}$. Introduce the function

$$\Phi(\zeta,u) = \begin{cases} \omega(\zeta), & (\zeta,u)\in\mathrm{C}_1,\\ \overline{\omega(\bar\zeta)}, & (\zeta,u)\in\mathrm{C}_2. \end{cases} \tag{3.2}$$

This function satisfies the symmetry condition $\overline{\Phi(\zeta_*,u_*)}=\Phi(\zeta,u)$, where $(\zeta_*,u_*)=(\bar\zeta,-u(\bar\zeta))$ is the point symmetric to a point $(\zeta,u(\zeta))$ with respect to the line l. Thus, if $(\zeta,u)\in\mathrm{C}_1$, then $(\zeta_*,u_*)\in\mathrm{C}_2$. On the symmetry line, the boundary values of the function $\Phi(\zeta,u)$ are

$$\Phi^+(\xi,v)=\omega(\xi) \quad\text{and}\quad \Phi^-(\xi,v)=\overline{\omega(\xi)}, \quad (\xi,v)\in l, \quad v=u(\xi). \tag{3.3}$$

This definition implies that the boundary values of the function $\Phi(\zeta,u)$ are linked by

$$\Phi^+(\xi,v)\pm\Phi^-(\xi,v)=\left(\log\left|\frac{\mathrm{d}w}{V_\infty\,\mathrm{d}z}\right|-\mathrm{i}\theta\right)\pm\left(\log\left|\frac{\mathrm{d}w}{V_\infty\,\mathrm{d}z}\right|+\mathrm{i}\theta\right). \tag{3.4}$$

Then, using the boundary conditions (2.4) and (2.5), we see that the function $\Phi(\zeta,u)$ must solve the following Riemann–Hilbert problem with a discontinuous coefficient on the surface $\mathcal{R}$.

Find all the functions $\Phi(\zeta,u)$ analytic in $\mathcal{R}\backslash l$, Hölder continuous up to the boundary l apart from the singular points a, a_0, b, c_0, c_1 and d with the boundary values satisfying the relation

$$\Phi^+(\xi,v)=G(\xi,v)\Phi^-(\xi,v)+g(\xi,v), \quad (\xi,v)\in l, \tag{3.5}$$

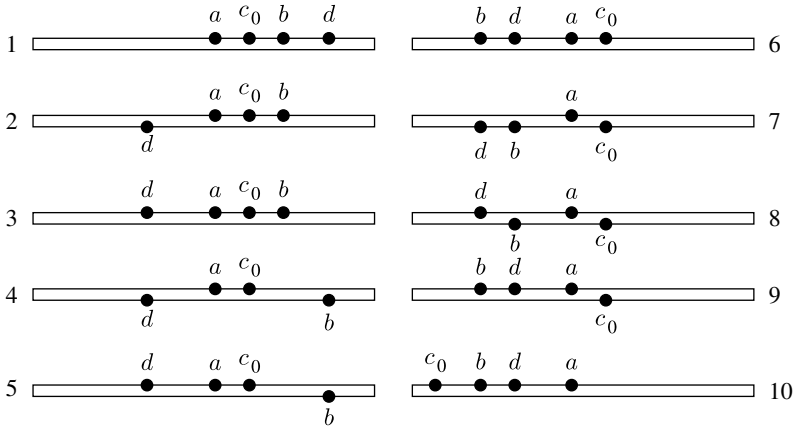

Figure 3. Possible cases for the canonical function $X(\zeta, u)$.

and the symmetry condition $\overline{\Phi(\zeta_*, u_*)} = \Phi(\zeta, u)$. Here,

$$G(\xi, v) = \begin{cases} -1, & (\xi, v) \in ac_0 \cup bc_1 d, \\ 1, & (\xi, v) \in da \cup c_0 b, \end{cases} \qquad g(\xi, v) = \begin{cases} 2\kappa_0', & (\xi, v) \in ac_0, \\ -2\mathrm{i}\alpha, & (\xi, v) \in c_0 b, \\ 2\kappa_1', & (\xi, v) \in bc_1 d, \\ 2\mathrm{i}(\pi - \beta), & (\xi, v) \in da_0, \\ -2\mathrm{i}\beta, & (\xi, v) \in a_0 a. \end{cases} \tag{3.6}$$

The function $\Phi(\zeta, u)$ has a logarithmic singularity at the point $(a_0, u(a_0))$, a square root singularity at the point $(c_0, u(c_0))$ and a simple pole at the point $(c_1, u(c_1))$. It is bounded at the points $(a, u(a))$, $(b, u(b))$ and $(d, u(d))$, and $\Phi(\zeta, u) \to 0$, $\zeta \to \infty$.

(*b*) *Canonical function*

To solve the Riemann–Hilbert problem, we need to find the canonical function, $X(\zeta, u)$, a solution to the following problem:

$$\begin{aligned} &X^+(\xi, v) = G(\xi, v) X^-(\xi, v), \quad X^+(\xi, v) = \overline{X^-(\xi, v)}, \quad (\xi, v) \in l, \\ &X(\zeta, u) = \overline{X(\bar{\zeta}, -u(\bar{\zeta}))}, \quad (\zeta, u) \in \mathcal{R} \backslash l. \end{aligned} \tag{3.7}$$

Such a function can be represented through a singular integral

$$X(\zeta, u) = K_0 \exp\left\{ \frac{1}{4\pi\mathrm{i}} \int_{\mathcal{L}} \log(-1) \left(1 + \frac{u}{v}\right) \frac{\mathrm{d}\xi}{\xi - \zeta} \right\}, \quad u = u(\zeta), \quad v = u(\xi). \tag{3.8}$$

Here, K_0 is a real constant to be chosen, $\mathcal{L} = ac_0 \cup bd$, and $\log(-1)$ is a branch of the logarithmic function to be specified. Clearly, the function $X(\zeta, u)$ is bounded at the infinite points of the surface and meets the symmetry condition (3.7). The function (3.8) can be found explicitly. Since a is fixed ($a = (1/2) + \mathrm{i}0$) and the points c_0, b and d follow each other in the clockwise direction, there are 10 possible cases (figure 3). Split the integral in (3.8) into two integrals

$$X(\zeta, u) = X_{ac_0}(\zeta, u) X_{bd}(\zeta, u), \tag{3.9}$$

where

$$X_{qr}(\zeta,u)=K_*\exp\left\{\frac{\sigma}{4}\int_{qr}\left(1+\frac{u}{v}\right)\frac{\mathrm{d}\xi}{\xi-\zeta}\right\}. \tag{3.10}$$

K_* is a real constant, $qr=ac_0$ or $qr=bd$, $\sigma=1$ if $\log(-1)$ is taken to be $\mathrm{i}\pi$ and $\sigma=-1$ in the case $\log(-1)=-\mathrm{i}\pi$. Evaluate the integral in (3.10) when $q=0$ and $r\in l^+$

$$I_+(r)=\int_{0r}\left(1+\frac{p^{1/2}(\zeta)}{p^{1/2}(\xi)}\right)\frac{\mathrm{d}\xi}{\xi-\zeta}=\int_0^r\frac{(1-\xi-\zeta)\mathrm{d}\xi}{\sqrt{\xi(1-\xi)}[\sqrt{\xi(1-\xi)}-\sqrt{\zeta(1-\zeta)}]}. \tag{3.11}$$

Make the substitutions $\xi_*=\sqrt{(1-\xi)/\xi}$, $\zeta_*=\sqrt{(1-\zeta)/\zeta}$ and $r_*=\sqrt{(1-r)/r}$, where ζ_* is the branch of the function $[(1-\zeta)/\zeta]^{1/2}$ fixed by the condition $\zeta_*\sim -i$ as $\zeta\to\infty$. This branch is a single-valued function in the ζ-plane with the cut l. Then, $\zeta_*=\pm|\zeta_*|$, $\zeta\in l^\pm$ and $\zeta_*=-\mathrm{i}|\zeta_*|$, $\zeta\in R\backslash[0,1]$. It can easily be shown that $I_+(r)$ transforms into

$$I_+(r)=-2\int_{r_*}^{\infty}\frac{(1+\zeta_*\xi_*)\mathrm{d}\xi_*}{(1+\xi_*^2)(\xi_*-\zeta_*)}=2\log\left(\sqrt{1-r}-\sqrt{r}\zeta_*\right), \tag{3.12}$$

where $\log(\cdot)$ is a fixed branch of the logarithmic function. When $r\in l^-$, the integral in (3.10), $I_-(r)$, can be evaluated similarly, $I_-(r)=2\log\left(\sqrt{1-r}+\sqrt{r}\zeta_*\right)$. Using these results, we can now find the function $X_{bd}(\zeta,u)$. There are five different cases (cases 1–5; figure 3) for the function X_{bd}. Choose $K_*=(b/d)^{1/4}$ and $\sigma=1$ in cases 1, 2, 4 and 5 and take $\sigma=-1$ in case 3. If $bd\subset l^+$ (cases 1, 6, 9 and 10; figure 3), then

$$X_{bd}(\zeta,u)=\left(\frac{b}{d}\right)^{1/4}\exp\left(\frac{I_+(d)}{4}-\frac{I_+(b)}{4}\right)=\sqrt{\frac{d_*-\zeta_*}{b_*-\zeta_*}}, \tag{3.13}$$

where $b_*=|\zeta_*(b)|$ and $d_*=|\zeta_*(d)|$. It is convenient to fix the arguments and therefore the branch of the function $\sqrt{(d_*-\zeta)/(b_*-\zeta)}$ in the following manner:

$$0\le\arg(d_*-\zeta_*)\le\pi\quad\text{and}\quad 0\le\arg(b_*-\zeta_*)\le\pi. \tag{3.14}$$

To complete the solution, we need the boundary values of the function X_{bd}^+ on the contour l. Since the function ζ_* maps the cut ζ-plane into the lower ζ_*-plane by using (3.14), we obtain

$$X_{bd}^+(\xi,v)=\begin{cases}\mathrm{i}|X_{bd}(\xi,v)|, & \xi\in bd,\\ |X_{bd}(\xi,v)|, & \xi\in l\backslash bd.\end{cases} \tag{3.15}$$

In a similar manner, we can write down the function $X_{bd}(\zeta,u)$ in the other cases as

$$X_{bd}(\zeta,u)=\begin{cases}\sqrt{(-d_*-\zeta_*)/(b_*-\zeta_*)}, & \text{case 2},\\ \mathrm{i}\sqrt{(d_*-\zeta_*)/(b_*-\zeta_*)}, & \text{case 3},\\ \sqrt{(-d_*-\zeta_*)/(-b_*-\zeta_*)}, & \text{cases 4 and 7},\\ \mathrm{i}\sqrt{(d_*-\zeta_*)/(-b_*-\zeta_*)}, & \text{cases 5 and 8},\end{cases} \tag{3.16}$$

where $0\le\arg(\pm d_*-\zeta_*)\le\pi$ and $0\le\arg(\pm b_*-\zeta_*)\le\pi$. Remarkably, the property (3.15) of the function $X_{bd}^+(\xi,v)$ is preserved in all the cases.

Now, analyse the function $X_{ac_0}(\zeta, u)$. Since the point a is fixed ($a=(1/2)+\mathrm{i}0$), there are only three distinct cases for the function X_{ac_0} (cases 1, 7 and 10; figure 3),

$$X_{ac_0}(\zeta,u)=\begin{cases}\sqrt{(c_*-\zeta_*)/(1-\zeta_*)}, & \text{cases 1 to 6,}\\ \sqrt{(-c_*-\zeta_*)/(1-\zeta_*)}, & \text{cases 7 to 9,}\\ \mathrm{i}\sqrt{(c_*-\zeta_*)/(1-\zeta_*)}, & \text{case 10,}\end{cases} \tag{3.17}$$

where $c_*=|\zeta_*(c)|$. The boundary value $X^+_{ac_0}(\xi, v)$ on the cut l is defined by (3.15), with b and d replaced by a and c_0, respectively.

(*c*) *Definition of the function* $\mathrm{d}w/\mathrm{d}z$

From (2.3) and (3.2), the derivative $\mathrm{d}w/\mathrm{d}z$ is expressed through the general solution

$$\Phi(\zeta,u)=X(\zeta,u)[\Psi(\zeta,u)+\Omega(\zeta,u)] \tag{3.18}$$

to the Riemann–Hilbert problem (3.5) in the form $(\mathrm{d}w/\mathrm{d}z)=V_\infty\exp\{\Phi(\zeta,u)\}$, $(\zeta,u)\in \mathrm{C}_1$. Here,

$$\Psi(\zeta,u)=\left(-\frac{\alpha}{2\pi}\int_{c_0b}-\frac{\beta}{2\pi}\int_{a_0a}+\frac{\pi-\beta}{2\pi}\int_{da_0}+\frac{\kappa_0'}{2\pi\mathrm{i}}\int_{ac_0}+\frac{\kappa_1'}{2\pi\mathrm{i}}\int_{bd}\right)\frac{(1+u/v)\mathrm{d}\xi}{X^+(\xi,v)(\xi-\zeta)}, \tag{3.19}$$

and $\Omega(\zeta, u)$ is a rational function on the surface $\mathcal{R}$. It is bounded at infinity and has simple poles at the points $\zeta=c_0$ and $\zeta=c_1$. The general form of such a function is given by

$$\Omega(\zeta,u)=M_0\frac{u(\zeta)+u(c_0)}{\zeta-c_0}+M_1\frac{u(\zeta)+u(c_1)}{\zeta-c_1}+M_2, \tag{3.20}$$

where M_j ($j=0, 1, 2$) are real constants to be fixed. It is directly verified that for any set of the constants M_j, the function (3.18) satisfies the symmetry condition $\overline{\Phi(\zeta_*,u_*)}=\Phi(\zeta,u)$. In general, however, the function (3.18) does not vanish at infinity as it is required. To meet this condition, find that $\Psi(\zeta,u)\sim\mathrm{i}\Psi_\infty$, $\zeta\to\infty$, where Ψ_∞ is real and

$$\Psi_\infty=\left(-\frac{\alpha}{2\pi}\int_{c_0b}-\frac{\beta}{2\pi}\int_{a_0a}+\frac{\pi-\beta}{2\pi}\int_{da_0}+\frac{\kappa_0'}{2\pi\mathrm{i}}\int_{ac_0}+\frac{\kappa_1'}{2\pi\mathrm{i}}\int_{bd}\right)\frac{\mathrm{d}\xi}{X^+(\xi,v)v}. \tag{3.21}$$

Next, note that for the branch chosen, $u(\zeta)\sim-\mathrm{i}\zeta$, $\zeta\to\infty$. Thus, for the function $\Phi(\zeta, u)$ being zero at infinity, it is necessary and sufficient that

$$\mathrm{i}\Psi_\infty-\mathrm{i}M_0-\mathrm{i}M_1+M_2=0, \tag{3.22}$$

and therefore $M_2=0$ and $M_0+M_1=\Psi_\infty$. The analysis of the function $X(\zeta, u)$ at the points a, a_0, b and d shows that it is bounded at the points c_0 and d but unbounded at the points a and b,

$$X(\zeta,u)=O((\zeta-e_1)^{-1/2}),\quad \zeta\to e_1 \text{ and } X(\zeta,u)=O((\zeta-e_2)^{1/2}),\quad \zeta\to e_2, \tag{3.23}$$

where $e_1=a, b$ and $e_2=c_0, d$. Owing to the smooth detachment of the cavities at the points $\zeta=a$, b and d, the solution $\Phi(\zeta, u)$ must be bounded at these points.

Clearly, the function (3.18) is bounded at the point $\zeta = d$ but not at the other two points. The boundedness is guaranteed if the constants M_0 and M_1 solve the following system:

$$\begin{gathered} \Psi_a + U(a, c_0)M_0 + U(a, c_1)M_1 = 0 \\ \text{and} \\ \Psi_b + U(b, c_0)M_0 + U(b, c_1)M_1 = 0, \end{gathered} \tag{3.24}$$

where

$$\Psi_h = \Psi(h, u(h)) \quad \text{and} \quad U(\zeta, \eta) = \frac{u(\zeta) + u(\eta)}{\zeta - \eta}. \tag{3.25}$$

Equations (3.22) and (3.24) define the constants M_0 and M_1 as

$$M_0 = \frac{\Psi_a + U(a, c_1)\Psi_\infty}{U(a, c_1) - U(a, c_0)} \quad \text{and} \quad M_1 = -\frac{\Psi_a + U(a, c_0)\Psi_\infty}{U(a, c_1) - U(a, c_0)}, \tag{3.26}$$

and also give an extra real equation for the unknown parameters

$$\Psi_b + U(b, c_0)\Psi_\infty + \frac{U(b, c_1) - U(b, c_0)}{U(a, c_0) - U(a, c_1)}[\Psi_a + U(a, c_0)\Psi_\infty] = 0. \tag{3.27}$$

(*d*) *Function* $\mathrm{d}w/\mathrm{d}\zeta$

In order to reconstruct the conformal mapping $f(\zeta)$, in addition to $\mathrm{d}w/\mathrm{d}z$, we need the derivative $\mathrm{d}w/\mathrm{d}\zeta$. Since $\mathrm{Im}(\mathrm{d}w/\mathrm{d}\zeta) = 0$ on l, the function $\mathrm{d}w/\mathrm{d}\zeta$ can be analytically continued by symmetry on the whole Riemann surface $\mathcal{R}$ of the algebraic function u defined in §3*a*. Then,

$$(\mathrm{d}w/\mathrm{d}\zeta)^+ - (\mathrm{d}w/\mathrm{d}\zeta)^- = 0, \quad (\zeta, u) \in l \subset \mathcal{R}. \tag{3.28}$$

By the generalized Liouville theorem, the solution of this Riemann–Hilbert problem is a rational function on the Riemann surface $\mathcal{R}$. This function is bounded at infinity. In the case when none of the points a_0, c_0 and c_1 coincide with the branch points of the surface, the rational function must have simple zeros at the points $(a_0, u(a_0))$ and $(c_1, u(c_1))$ and be bounded at the point $(c_0, u(c_0))$. On the sheet C_1, it has the form

$$\frac{\mathrm{d}w}{\mathrm{d}\zeta} = N\frac{\mathrm{d}w^\circ}{\mathrm{d}\zeta}, \quad \frac{\mathrm{d}w^\circ}{\mathrm{d}\zeta} = c_1 - a_0 + \frac{p^{1/2}(a_0)(\zeta - c_1) - p^{1/2}(c_1)(\zeta - a_0)}{p^{1/2}(\zeta)}, \tag{3.29}$$

where N is a real constant. This function vanishes at the points a_0 and c_1, and it is bounded at the point c_0.

4. Numerical algorithm

The conformal mapping $z=f(\zeta)$ can be found from (2.2) by integration. Since the mapping must be a single-valued function, we require

$$\int_{l_*} \frac{\partial f}{\partial \zeta} \mathrm{d}\zeta = 0, \tag{4.1}$$

where l_* is a simple closed contour (a circle for example) enclosing the cut l. We should also add the following two conditions that specify the distances between the points A and B and A and D:

$$\mathrm{B}-\mathrm{A} = \frac{N}{V_\infty}\Omega \quad \text{and} \quad \lambda_2 \sin\beta = \frac{N\Omega_2}{V_\infty}, \tag{4.2}$$

where

$$\Omega = \Omega_0 + \mathrm{i}\Omega_1 = \int_{\gamma(a,b)} \frac{\mathrm{d}w^\circ}{\mathrm{d}\zeta} \mathrm{e}^{-\omega(\zeta)} \mathrm{d}\zeta \quad \text{and} \quad \Omega_2 = \mathrm{Im} \int_{da} \frac{\mathrm{d}w^\circ}{\mathrm{d}\zeta} \mathrm{e}^{-\omega(\zeta)} \mathrm{d}\zeta. \tag{4.3}$$

Here, $\gamma(a,b)$ is a simple curve with the ending points a and b, which does not cross the cut l and does not pass through the point c_0. The conditions (4.2) give two real nonlinear conditions for the unknown parameters

$$\frac{\Omega_0}{\Omega_2} = \frac{\lambda_1 \cos\alpha}{\lambda_2 \sin\beta} \quad \text{and} \quad \frac{\Omega_1}{\Omega_2} = \frac{\lambda_1 \sin\alpha}{\lambda_2 \sin\beta} \tag{4.4}$$

and also define the constant $N = \Omega_2^{-1} V_\infty \lambda_2 \sin\beta$. For the five parameters of the conformal mapping, a_0, b, c_0, c_1 and d, we obtain three real nonlinear equations (3.27) and (4.4) and one complex equation (4.1).

In dealing with the system for the unknown parameters, it will be convenient to map the unit cut into the unit circle centred at $\zeta = 1/2$ and identify a boundary point e ($e = a, c_0, b, c_1, d, a_0$) by the polar angle $\theta(e)$. The point a has been fixed: $a = (1/2) + \mathrm{i}0$. Therefore, the nonlinear system has to be solved subject to the following constraint:

$$-\frac{3\pi}{2} < \theta(a_0) < \theta(d) < \theta(c_1) < \theta(b) < \theta(c_0) < \theta(a) = \frac{\pi}{2}. \tag{4.5}$$

Each point $\zeta = (\xi, i_\zeta)$ on the banks $l^\pm$ of the cut ($i_\zeta = \pm 1$, $\zeta \in l^\pm$) can be identified as follows:

$$\theta(\zeta) = \begin{cases} \theta_*, & i_\zeta = 1, \theta_* \le \pi/2, \\ -\theta_*, & i_\zeta = -1, \\ \theta_* - 2\pi, & i_\zeta = 1, \theta_* > \pi/2. \end{cases} \qquad \theta_* = \cos^{-1}(2\xi - 1), \tag{4.6}$$

To eliminate the constraints of (4.5), we introduce new variables (Trefethen 1980)

$$\tau_k = \log \frac{\theta_k - \theta_{k-1}}{\theta_{k+1} - \theta_k} \in (-\infty, \infty), \quad k = 1, 2, \ldots, 5. \tag{4.7}$$

Here, $\theta_0 = \theta(a) = (\pi/2)$, $\theta_1 = \theta(c_0)$, $\theta_2 = \theta(b)$, $\theta_3 = \theta(c_1)$, $\theta_4 = \theta(d)$, $\theta_5 = \theta(a_0)$ and $\theta_6 = -3\pi/2$. The coordinates θ_k are recovered from the following system of linear

equations:

$$(1+\tau_1^*)\theta_1-\tau_1^*\theta_2=\frac{\pi}{2},$$

$$-\theta_{k-1}+(1+\tau_k^*)\theta_k-\tau_k^*\theta_{k+1}=0,\quad k=2,\ldots,5$$

and

$$-\theta_4+(1+\tau_5^*)\theta_5=-\frac{3\pi\tau_5^*}{2}, \tag{4.8}$$

where $\tau_k^*=\exp\{\tau_k\}$, $k=1,\ldots,5$. This system can easily be solved explicitly and its solution is omitted. The nonlinear system for the new unknown parameters τ_k is solved by Newton's steepest descent method with the Jacobian matrix evaluated approximately.

The principal values of the singular integrals in (3.19) can be computed by using the following formula:

$$\int_{\delta_1}^{\delta_2}\frac{1}{2}\left(1+\frac{u(\xi)}{u(\tau)}\right)\frac{\mathrm{d}\tau}{X^+(\tau,u(\tau))(\tau-\xi)}=\frac{\pi}{n}\sum_{j=1}^{n}G(\tau_j,\xi),\quad \delta_1<\xi<\delta_2, \tag{4.9}$$

where $\tau_j=(1/2)(\delta_2+\delta_1)+(1/2)(\delta_2-\delta_1)\cos[(j-(1/2))\pi/n]$ and

$$G(\tau,\xi)=\frac{1}{\tau-\xi}\left[\left(1+\frac{u(\xi)}{u(\tau)}\right)\frac{\sqrt{(\delta_2-\tau)(\tau-\delta_1)}}{2X^+(\tau,u(\tau))}-\frac{\sqrt{(\delta_2-\xi)(\xi-\delta_1)}}{X^+(\xi,u(\xi))}\right]. \tag{4.10}$$

It is derived from the order n Gauss quadrature rule and the fact that the principal value of the Cauchy integral of the function $[(\delta_2-\tau)(\tau-\delta_1)]^{-1/2}$ over the segment (δ_1,δ_2) is equal to 0.

Next, determine the equations for the unknown boundaries of the nose bubble AC_0^+ and the upper and lower boundaries of a trailing cavity. Integrating the function (2.2) gives the upper and lower boundaries of the cavity

$$\left.\begin{aligned} z(\tau)&=\int_{b\tau}\frac{\mathrm{d}f}{\mathrm{d}\zeta}\mathrm{d}\zeta+\mathrm{B},\quad \tau\in bc_1\big(z\in\mathrm{BC}_1^+\big),\\ z(\tau)&=\int_{d\tau}\frac{\mathrm{d}f}{\mathrm{d}\zeta}\mathrm{d}\zeta+\mathrm{D},\quad \tau\in dc_1(z\in\mathrm{DC}_1^-).\end{aligned}\right\} \tag{4.11}$$

An equation for the partial cavity can be written similarly.

Finally, we derive an equation for the streamlines $\psi(x,y)=\mathrm{const}$. By using formula (3.29), we obtain

$$\begin{aligned}\psi^*(\zeta)=\mathrm{Im}\int_{a\zeta}\frac{\mathrm{d}w}{\mathrm{d}\zeta}\mathrm{d}\zeta=N\Bigg\{&(c_1-a_0)\mathrm{Im}\,\zeta+\Big[p^{1/2}(c_1)-p^{1/2}(a_0)\Big]\mathrm{Im}\sqrt{\zeta(1-\zeta)}\\&-\left[\left(a_0-\frac{1}{2}\right)p^{1/2}(c_1)-\left(c_1-\frac{1}{2}\right)p^{1/2}(a_0)\right]\log|\mathrm{i}(2\zeta-1)+2\sqrt{\zeta(1-\zeta)}|\Bigg\},\end{aligned} \tag{4.12}$$

where $\psi(x,y)\equiv\psi(z)=\psi^*(\zeta)$. This equation implicitly defines the image of the family of the streamlines.

5. Single cavity flow past a non-symmetric wedge

There are two possibilities to simplify the model proposed in §2. The first one is to assume that the nose bubble is so small that can be neglected. The deficiency of this model is the singularity of the velocity at the vertex of the wedge. The second model admits the ability of the wedge to turn around the vertex in the flow plane such that the flow branches at the vertex. In both the cases, there is only one trailing cavity and the number of the unknown parameters in the conformal mapping function is less than that in the original model.

Model I. If the partial cavity AC_0 is disregarded, then the points A and C_0 (and therefore the points a and c_0) coincide, $X(\zeta, u) = X_{bd}(\zeta, u)$ and the solution (3.18) to the Riemann–Hilbert problem (3.5) can be simplified. Since the canonical function $X(\zeta, u)$ is bounded at the point $\zeta = a$, the singularity of the function $\Phi(\zeta, u)$ is caused by the logarithmic singularity of the function $\Psi(\zeta, u)$, and the velocity has an integrable singularity at the vertex of the wedge

$$u_x + \mathrm{i}u_y = \frac{\overline{\mathrm{d}w}}{\mathrm{d}z} = V_\infty \overline{\exp\{\Phi(\zeta, u)\}} \sim K_0(\zeta - a)^{(\alpha-\beta)/\pi}, \quad \zeta \to a (z \to \mathrm{A}). \tag{5.1}$$

There are only four unknown parameters, b, c_1, d and a_0, that need to be recovered (the real parameter a can be chosen arbitrarily).

Model II. This model assumes that the vertex A of the wedge is fixed but the wedge itself may rotate through an angle δ about the axis passing through the point A and orthogonal to the flow domain. The angle δ is not prescribed and is to be determined from the condition that the flow branches at the vertex of the wedge. In this case, there is no partial cavity AC_0 and points A and A_0 coincide. This means that $a = a_0 = c_0$ and the formulae for the solution are simplified further. The canonical function $X(\zeta, u)$ is the same as in model I, $X(\zeta, u) = X_{bd}(\zeta, u)$, and the functions Ω and Ψ are given by

$$\left.\begin{aligned} \Omega(\zeta, u) &= M_1 \frac{u(\zeta) + u(c_1)}{\zeta - c_1} + M_2 \\ \text{and} \\ \Psi(\zeta, u) &= \left(-\frac{\alpha}{2\pi} \int_{ab} + \frac{\pi - \beta}{2\pi} \int_{da} + \frac{\kappa_1'}{2\pi \mathrm{i}} \int_{bd} \right) \frac{(1 + u/v)\mathrm{d}\xi}{X^+(\xi, v)(\xi - \zeta)}. \end{aligned}\right\} \tag{5.2}$$

In contrast to model I, the angles α and β are not fixed: $\alpha = \alpha_0 + \delta$ and $\beta = \beta_0 + \delta$, where α_0 and β_0 are the prescribed angles that define the initial position of the wedge and δ is the angle of rotation of the wedge to be determined. To fix this angle, represent the function (5.2) as follows:

$$\Psi(\zeta, u) = \Psi^0(\zeta, u) + \delta \Psi^1(\zeta, u), \tag{5.3}$$

where $\Psi^0(\zeta, u)$ coincide with $\Psi(\zeta, u)$ if α_0 and β_0 are replaced by α and β, respectively. The function Ψ^1 is given by

$$\Psi^1(\zeta, u) = -\frac{1}{2\pi} \int_{dab} \frac{(1 + u/v)\mathrm{d}\xi}{X^+(\xi, v)(\xi - \zeta)}. \tag{5.4}$$

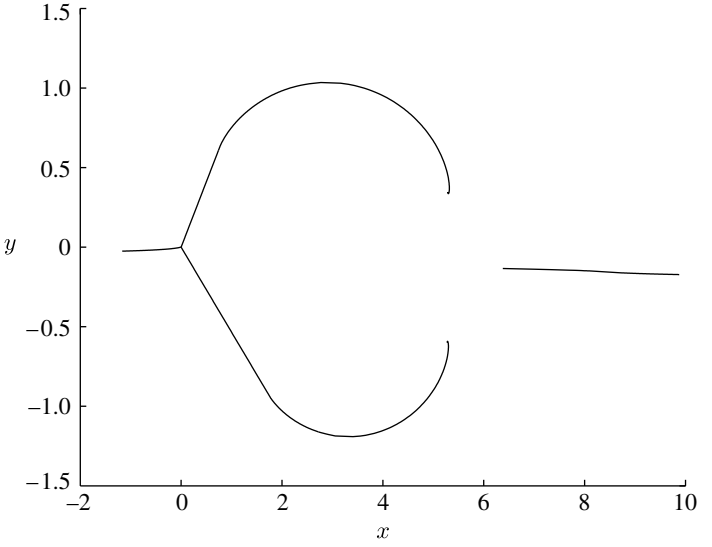

Figure 4. Single cavity flow past a wedge: $\kappa_1 = 1$, $\lambda_1 = 1$, $\lambda_2 = 2$, $\alpha_0 = \pi/8$ and $\beta_0 = 3\pi/4$.

As in model I, the solution to the Riemann–Hilbert problem (3.5) must be bounded at the point $\zeta = b$ and vanish at infinity. By using the representation (5.3), these conditions can be rewritten in the form

$$M_1 = \Psi_\infty, \quad M_2 = 0 \quad \text{and} \quad \delta = -\frac{\Psi_b^0 + U(b, c_1)\Psi_\infty^0}{\Psi_b^1 + U(b, c_1)\Psi_\infty^1}, \tag{5.5}$$

where $\Psi_b^j = \Psi^j(b, u(b))$; Ψ_∞^0 coincides with Ψ_∞ if α and β are replaced by α_0 and β_0, respectively; and

$$\Psi_\infty^1 = -\frac{1}{\pi}\int_{dab} \frac{\mathrm{d}\xi}{X^+(\xi, v)v}. \tag{5.6}$$

The nonlinear system for the unknown parameters consists of one real equation and one complex equation

$$\frac{\Omega_1}{\Omega_2} = \frac{\lambda_1 \sin\alpha}{\lambda_2 \sin\beta} \quad \text{and} \quad \int_0^{2\pi} \left.\frac{\partial f}{\partial \zeta}\right|_{\zeta = 1/2 + r\,\exp\{\mathrm{i}\theta\}} \mathrm{e}^{\mathrm{i}\theta}\,\mathrm{d}\theta = 0 \quad \left(r \geq \frac{1}{2}\right). \tag{5.7}$$

As before, we fix $a = (1/2) + \mathrm{i}0$ and find the remaining three parameters b, c_1 and d from this system by the scheme of §4.

In figure 4, the shape of the cavity is plotted for the case when the cavitation number $\kappa_1 = 1$, the lengths of the wedge sides are different, $\lambda_1 = 1$ and $\lambda_2 = 2$, and the initial angles that the wedge makes with the positive real semi-axis are $\alpha_0 = \pi/8$ and $\beta_0 = 3\pi/4$. In this case, the Newton scheme gives the accuracy of 10^{-7} after five iterations. The unknown parameters of the conformal mapping for the chosen value $a = 0.5 + \mathrm{i}0$ become $b = 0.816957 + \mathrm{i}0$, $c_1 = 0.475976 - \mathrm{i}0$ and $d = 0.071019 + \mathrm{i}0$. The angle of rotation is $\delta = 0.294750$. To recover a streamline $\psi(x, y) \equiv \psi^*(\xi, \eta) = 0$, we first use the Newton scheme to define ξ as a function of η in the form

$$\xi_{n+1} = \xi_n - \frac{\psi^*(\xi_n, \eta)}{\psi_\xi^*(\xi_n, \eta)}, \quad n = 0, 1, \ldots, \tag{5.8}$$

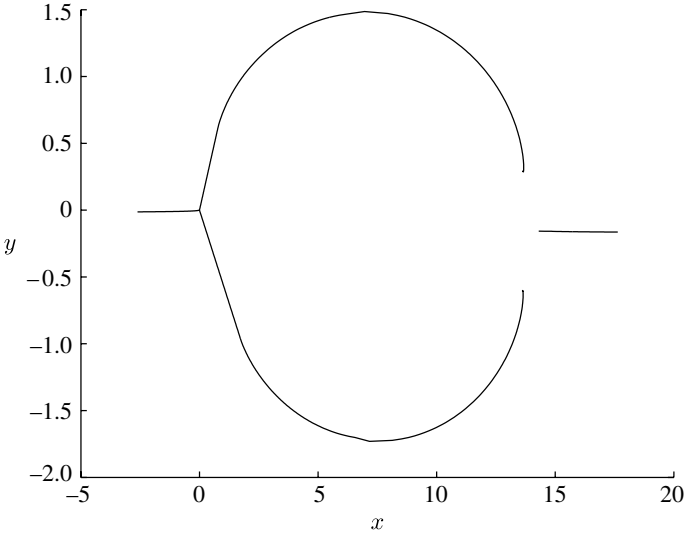

Figure 5. Single cavity flow past a wedge: $\kappa_1 = 0.5$, $\lambda_1 = 1$, $\lambda_2 = 2$, $\alpha_0 = (\pi/8)$ and $\beta_0 = (3\pi/4)$.

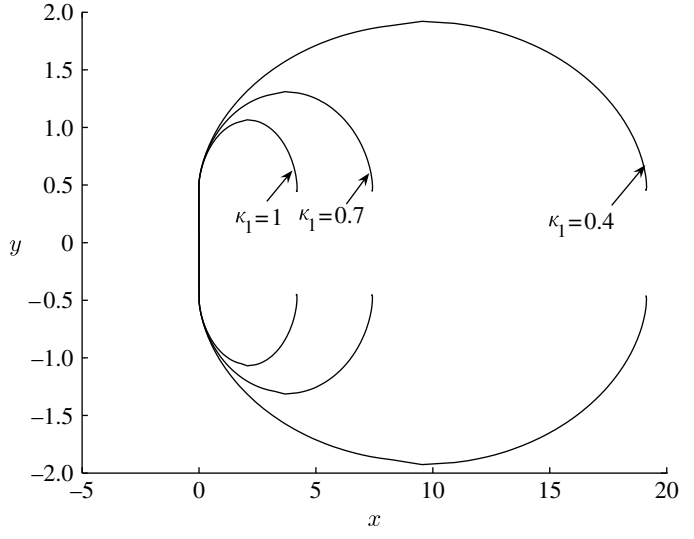

Figure 6. The cavity behind a plate: the symmetric case. The parameters are $\kappa_1 = 0.4$, $\kappa_1 = 0.7$ or $\kappa_1 = 1$, $\alpha_0 = \beta_0 = \pi/2$ and $\lambda_1 = \lambda_2 = 0.5$.

and then integrate the function $\mathrm{d}f/\mathrm{d}\zeta$ either over a curve ap, or a curve abc_1q to obtain

$$z = \int_{ap} \frac{\mathrm{d}f}{\mathrm{d}\zeta}\mathrm{d}\zeta,\ z \in \mathrm{AP} \quad \text{and} \quad z = \int_{c_1 q} \frac{\mathrm{d}f}{\mathrm{d}\zeta}\mathrm{d}\zeta + \mathrm{C}_1,\ z \in \mathrm{C}_1\mathrm{Q}, \tag{5.9}$$

where $\mathrm{C}_1 = (\mathrm{C}_1^+ + \mathrm{C}_1^-)/2$, $\mathrm{P} = f(p)$ and $\mathrm{Q} = f(q)$. In figure 4, we plot the streamline $\psi(x, y) = 0$ that branches at the vertex A, flows around the wedge and defines the shape of the cavity. Another example of the shape of the cavity

Table 1. Dimensionless length L' and width H' of the cavity for a foil for some values of the cavitation number κ_1.

κ_1	L'	L' (Gurevich 1979)	H'	H' (Gurevich 1979)
0.4	19.116	19.1190	3.805	3.7962
0.7	7.398	7.4076	2.598	2.5942
1.0	4.172	4.1851	2.115	2.1131

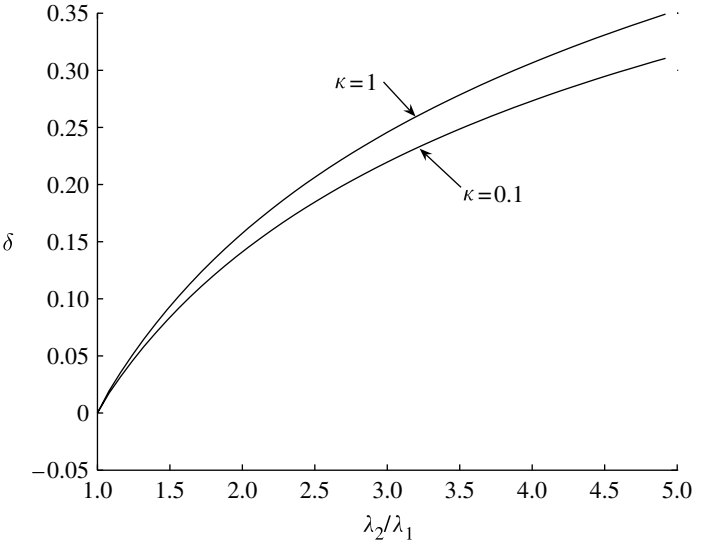

Figure 7. The angle of rotation δ versus the ratio λ_2/λ_1 for $\kappa_1 = 0.1$ and $\kappa_1 = 1$ when $\alpha_0 = \pi/3$ and $\beta_0 = 2\pi/3$.

and the branched streamline $\psi(x, y) = 0$ is shown in figure 5. In this case, $\kappa_1 = 0.5$, $\lambda_1 = 1$, $\lambda_2 = 2$, $\alpha_0 = (\pi/8)$ and $\beta_0 = (3\pi/4)$. The size of the cavity grows when the cavitation number decreases. For the symmetric case when $\alpha_0 = \beta_0 = (\pi/2)$, the wedge becomes a foil and the angle of rotation $\delta = 0$. In figure 6, we show the cavities for some values of the cavitation number. Our computations of the dimensionless length $L' = L/\lambda$ and width $H' = H/\lambda$ ($\lambda = \lambda_1 + \lambda_2$) of the cavity are in good agreement with the corresponding values L' and H' obtained by Gurevich (1979) (table 1).

The dependence of the angle of rotation δ on the ratio λ_2/λ_1 of the lengths of the wedge sides is illustrated in figure 7. The angle increases when the cavitation number increases.

6. Conclusions

In the present paper, we have analysed the potential flow around a non-symmetric wedge using a double and a single cavity model. Based on the general theory of conformal mappings, it has been shown that the number of unknown constants and the number of additional conditions coincide if both the cavities,

the nose bubble and the trailing cavity are modelled by the Tulin single-vortex scheme. To recover the actual form of the conformal mapping function, we have solved the two Riemann–Hilbert problems on the same genus-zero Riemann surface. The final form of the conformal map possesses five unknown parameters. It turns out that the Newton scheme developed for the solution of the system of transcendental equations for the parameters is sensitive to the data: the two cavitation numbers, κ_0 and κ_1; the ratio of the lengths of the wedge sides, λ_2/λ_1; and the angles α and β. This circumstance can be caused by the branch points of the Riemann surface (the numerical scheme is not stable when the parameters approach the branch points). Another reason for this could be the existence of the singularity of the solution at the point C_0, where the streamline attempts to join the upper side of the wedge forming a nose bubble. It is more likely that the nose bubble is thin, and therefore the fact that $\omega(\zeta) \sim K(\zeta - c_0)^{-1/2}$ as $\zeta \to c_0$ may be not the best way to model the closure mechanism of the partial cavity in the double cavity flow. The removal of this singular point from the model, however, creates a cusp at the point C_0 and, in addition, breaks the balance between the number of the unknown parameters and the number of conditions, and the solution does not exist. At the same time, the use of a linearized model for the partial cavity and the nonlinear model for the trailing cavity leads to the following nonlinear problem:

$$\begin{gathered}
\operatorname{Im} w(z) = K, \quad z \in L_0 \cup \mathrm{C_0B} \cup L_1 \cup \mathrm{DA}, \quad K = \text{const.}, \\
u_x = V_\infty \sqrt{1+\kappa_0}, \quad z \in L_0, \qquad u_x^2 + u_y^2 = V_\infty^2 (1+\kappa_1), \quad z \in L_1, \\
u_x \sin\alpha - u_y \cos\alpha = 0, \quad z \in \mathrm{C_0B} \quad \text{and} \quad u_x \sin\beta - u_y \cos\beta = 0, \quad z \in \mathrm{AD}.
\end{gathered} \tag{6.1}$$

Here, α is small and $(u_y/V_\infty)^2 \sim 0$, $z \in L_0$. To the best of our knowledge, such a nonlinear problem has never been considered in the literature.

In the case when the wedge is allowed to rotate about the vertex in the flow domain, the flow branches at the vertex. In this case, we described the flow by the Tulin single-vortex model. The number of unknowns decreases to 3, and the Newton scheme for the solution of the system of nonlinear equations for the unknown parameters is stable and demonstrates a good rate of convergence. We managed to reconstruct the actual form of the conformal mapping function and the branched streamline.

In our future publication, we shall develop another method based on a conformal mapping of the exterior of n ($n \geq 1$) discs onto the flow domain. For $n \geq 2$, the method requires the solution of the two Riemann–Hilbert problems of the theory of automorphic functions. Although it produces a closed-form solution (by quadratures) only in the simply connected case and represents the solution in terms of sequences of series and products in the case $n \geq 2$, it has two advantages. First, the numerical problem associated with the branch points of the Riemann surface is avoided and, second, the solution of the Jacobi problem ($n \geq 2$) can be bypassed.

This work was funded by the NSF through grant DMS0707724, the Louisiana Board of Regents through grant LEQSF(2005-07)-ENH-TR-09 and the Russian Foundation for Basic Research through grant 07-01-00038. The authors thank Dr S. A. Kinnas for useful discussions of the results.

References

Antipov, Y. A. & Silvestrov, V. V. 2007 Method of Riemann surfaces in the study of supercavitating flow around two hydrofoils in a channel. *Physica D* **235**, 72–81. (doi:10.1016/j.physd.2007.04.013)

Birkhoff, G. & Zarantello, E. H. 1957 *Jets, wakes, and cavities*. New York, NY: Academic Press.

Brennen, C. E. 1995 *Cavitation and bubble dynamics*. Oxford, UK: Oxford University Press.

Cherepanov, G. P. 1964 Flow of an ideal fluid with free surface in doubly connected and triply connected regions. *J. Appl. Math. Mech.* **27**, 1117–1124. (doi:10.1016/0021-8928(63)90193-X)

Cox, A. D. & Clayden, W. A. 1958 Cavitating flow about a wedge at incidence. *J. Fluid Mech.* **3**, 615–637. (doi:10.1017/S0022112058000227)

Eisenberg, P. & Tulin, M. P. 1961 Cavitation. In *Handbook of fluid dynamics* (ed. V. L. Streeter), pp. 12-1–12-46. New York: McGraw-Hill.

Frank, J.-P. & Michel, J.-M. 2004 *Fundamentals of cavitation*. New York, NY: Kluwer Academic Publishers.

Gurevich, M. I. 1979 *The theory of jets in an ideal fluid*. Moscow, Russia: Nauka.

Terent'ev, A. G. 1976 Non-linear theory of cavitational flow around obstacles. *Fluid Dyn.* **11**, 142–145. (doi:10.1007/BF01023411)

Trefethen, L. N. 1980 Numerical computation of the Schwarz–Christoffel transformation. *SIAM J. Sci. Stat. Comput.* **1**, 82–102. (doi:10.1137/0901004)

Tulin, M. P. 1964 Supercavitating flows—small perturbation theory. *J. Ship Res.* **7**, 16–37.

Wu, T. Y. 1972 Cavity and wake flows. *Annu. Rev. Fluid Mech.* **4**, 243–284. (doi:10.1146/annurev.fl.04.010172.001331)